Formation of Crystalline Germanium Nanoclusters in a Silica Xerogel Matrix from an Organogermanium Precursor

Joseph P. Carpenter and C. M. Lukehart*

Department of Chemistry, Vanderbilt University, Nashville, Tennessee 37235

D. O. Henderson and R. Mu

Physics Department, Fisk University, Nashville, Tennessee 37208

Bobby D. Jones and R. Glosser

Department of Physics, University of Texas at Dallas, Richardson, Texas 75083

S. R. Stock

School of Materials Science and Engineering, Georgia Institute of Technology, Atlanta, Georgia 30332

James E. Wittig

Department of Applied & Engineering Sciences, Vanderbilt University, Nashville, Tennessee 37235

Jane G. Zhu

Solid-State Division, Oak Ridge National Laboratory, Oak Ridge, Tennessee 37831

Received November 16, 1995. Revised Manuscript Received March 18, 1996[⊗]

Addition of the organogermanium compound, $Me_3GeS(CH_2)_3Si(OMe)_3$, to a modified, conventional sol−gel formulation gives a silica xerogel doped with this molecular species. Subsequent thermal treatment of this molecularly doped xerogel under oxidizing then reducing conditions affords nanoclusters of Ge highly dispersed throughout the bulk of the xerogel matrix. Under appropriate conditions, Ge nanoclusters having an average diameter of ca. 68 Å can be formed by this procedure. Characterization of this nanocomposite material by TEM, HRTEM, EDS, XRD, micro-Raman spectroscopy, electron diffraction, and UV−visible spectroscopy indicates that the Ge nanoclusters are highly crystalline and exhibit optical properties consistent with those expected when quantum confinement effects are operative.

Introduction

Nanocomposite materials consisting of very small particles of a guest substance (typically having diameters less than 100 nm) dispersed throughout a host matrix are of intense current interest for potential applications in chemical catalysis or as magnetic, electronic, or photonic materials.[1−6] Nanocrystalline particles of semiconductor substances, commonly referred to as quantum dots or Q-particles, exhibit new quantum phenomena which have potential application in a variety of photonic devices.[1−7] Although direct bandgap semiconductors, such as CdS or CdSe, have been studied extensively, the recent discovery of photoluminescence from nanoparticles of indirect bandgap semiconductors, such as Si or Ge, has generated much interest in these materials.[9−16]

Nanocrystalline particles of Ge have been prepared by several methods. Several groups have used the rf-magnetron cosputtering of Ge and SiO_2 onto Si substrates to produce thin films containing nanoparticulate Ge embedded within a silica matrix.[13,14,17−19] An aver-

* To whom correspondence should be addressed.

[⊗] Abstract published in *Advance ACS Abstracts,* May 1, 1996.

(1) Stucky, G. D. *Naval Res. Rev.* **1991**, *43*, 28.
(2) Sinfelt, J. H.; Meitzner, G. D. *Acc. Chem. Res.* **1993**, *26*, 1.
(3) Steigerwald, M. L.; Brus, L. E. *Acc. Chem. Res.* **1990**, *23*, 183.
(4) Wang, Y. *Acc. Chem. Res.* **1991**, *24*, 133.
(5) Weller, H. *Angew. Chem., Int. Ed. Engl.* **1993**, *32*, 41.
(6) Weller, H. *Adv. Mater.* **1993**, *5*, 88.
(7) Brus, L. *IEEE J. Quantum Electron.* **1986**, *QE-22*, 1909.
(8) Brus, L. *Appl. Phys.* **1991**, *A53*, 465.
(9) Cullis, A. G.; Canham, L. T. *Nature* **1991**, *353*, 335.
(10) Canham, L. T. *Appl. Phys. Lett.* **1990**, *57*, 1046.
(11) Furukawa, S.; Miyasato, T. *Phys. Rev.* **1988**, *B38*, 5726.
(12) Paine, D. C.; Caragianis, C.; Kim, T. Y.; Shigesto, Y.; Ishahara, T. *Appl. Phys. Lett.* **1993**, *62*, 2842.
(13) Kanemitsu, Y.; Uto, H.; Masumoto, Y.; Maeda, Y. *Appl. Phys. Lett.* **1992**, *61*, 2187.
(14) Maeda, Y.; Tsukamoto, N.; Yazawa, Y.; Kanemitsu, Y.; Masumoto, Y. *Appl. Phys. Lett.* **1991**, *59*, 3168.
(15) Tomiya, S.; Petroff, P. M.; Margolese, D.; Srdanov, V. I.; Stucky, G. D.; Zhang, Y. H. *Mater. Res. Soc. Symp.* **1993**, *286*, 353.
(16) Brus, L. E.; Szajowski, P. F.; Wlson, W. L.; Harris, T. D.; Schuppler, S.; Citrin, P. H. *J. Am. Chem. Soc.* **1995**, *117*, 2915.
(17) Fujii, M.; Hayashi, S.; Yamamoto, K. *Jpn. J. Appl. Phys.* **1991**, *30*, 687.
(18) Fujii, M.; Hayashi, S.; Yamamoto, K. *Appl. Phys. Lett.* **1990**, *57*, 2692.
(19) Hayashi, S.; Fujii, M.; Yamamoto, K. *Jpn. J. Appl. Phys.* **1989**, *28*, L 1464.

S0897-4756(95)00548-5 CCC: $12.00

age Ge particle size of 4−14 nm is obtained depending on the Ge:SiO_2 volume ratio and annealing temperature used in the synthesis. Caragianis and co-workers have prepared thin films of Si/Ge on a Si substrate. Sequential hydrothermal oxidation and reduction by hydrogen produced nanoparticulate Ge having average diameters of 3−5 nm within a SiO_2 matrix.[12,21] Carles and co-workers formed Ge/carbon films by chemical vapor deposition (CVD) of tetraorganogermanes onto Si substrates.[20] Germanium grains up to 55 nm in average diameter are produced. Nanoparticulate Ge embedded within a GeO_2 matrix has been prepared by Ovsyuk and co-workers via the thermal disproportionation of GeO on sapphire.[22] Particle sizes ranged from 7 to 24 nm. Relatively large particles of Ge (average diameter of 2000 Å) have been prepared by Stucky and co-workers from the thermal vapor decomposition of GeH_4 inside proton-exchanged zeolite Y.[15] A solution-phase synthesis of Ge colloids involving reduction of germanium halide compounds with a Na−K dispersion followed by a high-pressure treatment at elevated temperature to ensure crystallization of the colloids has been reported recently by Alivisatos and co-workers.[23] This latter method involves dangerous experimental procedures. The synthetic method reported herein represents a complementary strategy for the preparation of Ge nanocomposite materials using sol−gel chemistry. Nanoparticulate Ge embedded within a silica xerogel matrix is readily prepared using standard sol−gel synthetic techniques and subsequent thermal processing. While the germanium nanocomposites discussed below are prepared as bulk powders for convenience, sol−gel techniques should also permit formation of these nanocomposites as thin films or monoliths.

We now report the successful formation of Ge nanoparticles (average size of ca. 68 Å) as nanoclusters of Ge highly dispersed throughout a bulk silica xerogel matrix. This nanocomposite material is prepared by subjecting a silica xerogel doped with a single-source molecular precursor to successive oxidative and reductive thermal treatments. The molecular precursor, $Me_3GeS(CH_2)_3Si(OMe)_3$, is an organogermanium compound containing a bifunctional thiolate substituent. Addition of this germanium compound to a conventional sol−gel formulation gives covalent incorporation of this organogermanium molecular precursor into the resulting silica xerogel matrix via the hydrolysis and subsequent condensation reactions of the trialkoxysilyl functional group. The resulting Ge nanocomposite has been characterized by transmission electron microscopy (TEM), high-resolution TEM, energy-dispersive spectroscopy (EDS), electron diffraction, X-ray diffraction (XRD), micro-Raman spectroscopy, UV−visible transmission spectroscopy, and chemical microanalysis. A discussion of this general synthetic strategy as a method for preparing a variety of nanocomposite materials has been reported.[24]

Experimental Section

Reagents and Methods. The reagents, tetramethylorthosilicate (TMOS) and (3-mercaptopropyl)trimethoxysilane, were purchased from Aldrich Chemical Co., Inc. Silica xerogels were formed at 25 °C using standard sol−gel formulations with minor modification of the procedure reported by Sakka.[25,26] All operations were performed at room temperature unless otherwise specified.

Proton NMR spectra were recorded on a IBM NR-300 spectrometer (300 MHz) using the ^2H signal of the solvent as an internal lock frequency. Chemical shifts (in δ) were measured with respect to the residual solvent peak as an internal standard.

Nanocomposite materials were characterized by using a Philips CM20T transmission electron microscopy (TEM) operating at 200 kV. Samples for TEM were prepared by dispersing a powdered sample of nanocomposite onto a 3-mm diameter copper grid covered with amorphous carbon as a substrate. These samples were analyzed with standard bright-field (BF) imaging for particle-size distribution, selected area diffraction (SAD) for their crystal structures, and X-ray energy-dispersive spectroscopy (EDS) for semiquantitative chemical composition. High-resolution TEM (HRTEM) micrographs were obtained on a Hitachi HF 2000 transmission electron microscope.

X-ray diffraction (XRD) scans were obtained using a Philips PW1800 $\theta/2\theta$ automated powder diffractometer equipped with a Cu target and a post-sample monochromator. Samples for XRD were prepared by placing a uniform layer of powdered nanocomposite onto double-sided tape affixed to the sample holder. The sample area was greater than the ca. 1 cm × 1 cm area irradiated by the X-ray beam. Considerable caution was used to keep the top of the sample surface flat and coplanar with the diffractometer rotation axis. An initial XRD scan over the angular range 20−60° 2θ (in angular increments of 0.03° 2θ and a counting time of 1 s/step) confirmed the presence of the 111, 220, and 311 diffraction peaks of Ge and no other crystalline phases. To improve the signal-to-noise ratio of these three diffraction peaks, each peak was scanned again using a step size of 0.15° 2θ and a counting time of 80 s. Prior to peak width measurement, each diffraction peak was corrected for background scattering and was stripped of the Kα_2 portion of the diffracted intensity. The full width at half-maximum (fwhm) was measured for each peak. Crystallite size, L, was calculated from Scherrer's equation, $L = K\lambda/\beta \cos\theta_B$, for peak broadening from size effects only (where β is the peak fwhm measured in radians on the 2θ scale, λ is the wavelength of X-rays used, θ_B is the Bragg angle for the measured *hkl* peak, and K is a constant equal to 1.00 for L taken as the volume-averaged crystallite dimension perpendicular to the *hkl* diffraction plane).[27]

Micro-Raman spectra were recorded on an Instruments SA U1000 spectrometer equipped with a 1-m double monochromator with a pair of 1800 grooves/mm holographic gratings. The excitation source used was the 476.5 nm line from a Lexel Model 95 argon-ion laser. Plasma lines from the laser were removed using a Pellin Broca prism. An Olympus microscope having 50× or 100× objectives was attached to the monochromator. The minimum laser spot diameter was 1 μm in diameter, and, with a beam power of approximately 4 mW, the laser intensity at the sample was approximately 0.5 MW/cm^2. A thermoelectrically cooled Hamamatsu GaAs photomultiplier tube served as the detector. All data collection and analysis was automated.

Thermogravimetric analysis (TGA) was performed on a Seiko Instruments TG/DTA 220 instrument. A sample of the molecularly doped xerogel was heated in air from 25 to 900 °C at a rate of 10 °C/min. Sample mass was referenced to that

(20) Carles, R.; Mlayah, A.; Amjoud, M.; Reynes, A.; Morancho, R. *Jpn. J. Appl. Phys.* **1992**, *31*, 3511.
(21) Paine, D. C.; Kim, T. Y.; Caragianis, C.; Shigesato, Y. *J. Electron. Mater.* **1994**, *23*, 901.
(22) Ovsyuk, N. N.; Gorokhov, E. B.; Grishchenko, V. V.; Shebanin, A. P. *JETP Lett.* **1988**, *47*, 298.
(23) Heath, J. R.; Shiang, J. J.; Alivisatos, A. P. *J. Chem. Phys.* **1994**, *101*, 1607.
(24) Lukehart, C. M.; Carpenter, J. P.; Milne, S. B.; Burnam, *Chemtech* **1993**, *23*, Issue No. 8, 29.
(25) Brinker, C. J.; Scherer, G. W. *Sol-Gel Science*; Academic Press: New York, 1990.
(26) Adachi, T.; Sakka, S. *J. Mater. Sci.* **1987**, *22*, 4407.
(27) Klug, H. P.; Alexander, L. E. *X-Ray Diffraction Procedures for Polycrystalline and Amorphous Materials*, 2nd ed.; John Wiley & Sons: New York, 1974.

of an empty pan. Microanalyses were performed by Galbraith Laboratories, Inc., Knoxville, TN.

Optical spectra were recorded with a Hitachi 3501 double-beam spectrometer equipped with a 60-mm Hitachi integrating sphere fitted with a photomultiplier and a cooled PbS detector. With this optical configuration, transmission measurements were made in the region between 240 and 2600 nm. All optical measurements were made at a resolution of 0.5 nm. Repeated measurements showed the photometric accuracy to be ±0.8% transmittance and ±0.7 nm in wavelength accuracy. Samples for optical measurements were prepared by dispersing the powdered nanocomposite in EPO-TEK 302 (an optical epoxy resin obtained from Epoxy Technology, Inc., Billerica, MA). This dispersion was then permitted to harden between two glass slides giving a xerogel/epoxy matrix. The refractive index of this epoxy resin of 1.5661 is similar to that of highly densified silica xerogels[25] and thus provides index matching within the sample to reduce light scattering.

Preparation of $Me_3GeS(CH_2)_3Si(OMe)_3$ (1). Compound **1** was prepared from Me_3GeBr, $HS(CH_2)_3Si(OMe)_3$, and NEt_3 following a general procedure reported by Mehrotra and co-workers for related compounds.[28] To a solution of 4.97 g (25.3 mmol) of $HS(CH_2)_3Si(OMe)_3$ in 50 mL of benzene was added 2.66 g (26.3 mmol) of NEt_3. To this stirred solution was added dropwise 5.0 g (25.3 mmol) of Me_3GeBr over 30 min. During this addition, a white precipitate was formed. After an additional 2 h, the reaction mixture was filtered through Celite, and the solvent was removed from the filtrate at reduced pressure, giving 7.8 g (98% yield) of $Me_3GeS(CH_2)_3Si(OMe)_3$ as a crude, viscous liquid. Distillation (97−100 °C, 10 mmHg) of this product yielded 6.3 g (80% yield) of **1** as a colorless liquid: ^{1}H NMR ($CDCl_3$) δ 0.52 (s, 9H, *Me*$_3$Ge), 0.78 (m, 2H, *CH*$_2$Si), 1.71 (m, 2H, *CH*$_2$CH$_2$Si), 2.54 ("t", 2H, "$^3J_{HH}$" = 7 Hz, S*CH*$_2$), 3.57 (s, 9H, O*Me*$_3$). Anal. Calcd for $C_9H_{24}GeO_3SSi$: C, 34.53; H, 7.73. Found: C, 34.13; H, 7.30.

Typical Preparations of Silica Xerogels Containing Covalent Incorporation of $Me_3GeS(CH_2)_3Si(OMe)_3$ (1) Using Either Base or Acid Catalysis. *Xerogel Obtained from a 3:1 Total Si:Ge Reactant Molar Ratio Using Base Catalysis* ***(2a).*** A vial was charged with 263 mg (0.84 mmol) of **1**, 0.25 mL (1.68 mmol) of TMOS, 0.24 mL (3.1 mmol) of dimethylformamide (DMF), and 0.38 mL (21 mmol) of water. The cloudy mixture was made homogeneous by the addition of 0.80 mL of methanol. While the solution was being stirred magnetically, 0.05 mL of 0.148 M NH_3 was added. After 20 min the resulting sol set up as a clear wet gel. Three days after gelation, the gel was fractured and was removed from the vial, and the remaining methanol was allowed to evaporate. The gel was then washed with 3 × 5 mL of methanol and then dried in vacuo for 30 min to yield 297 mg of apparently dry, clear, colorless xerogel fragments. Anal. C, 13.43; H, 3.05; S, 7.47; Ge, 6.22; Si, 29.01.

Xerogel Obtained from a 10:1 Total Si:Ge Reactant Molar Ratio Using Acid Catalyst ***(3a).*** A vial was charged with 117 mg (0.374 mmol) of **1**, 0.50 mL (3.36 mmol) of TMOS, 0.28 mL (3.74 mmol) of DMF, and 0.66 mL (37.4 mmol) of water. The cloudy mixture was made homogeneous by the addition of 0.45 mL of methanol. While the solution was being stirred magnetically, 0.05 mL of 1.2 M HCl was added. After a 24 h gelation time, the resulting sol set up as a wet gel. Two days after gelation, the gel was fractured and was removed from the vial. The excess solvent was allowed to evaporate, and the gel was washed with 3 × 10 mL of methanol. The gel was dried in vacuo for 30 min to yield 298 mg of apparently dry, clear, colorless xerogel fragments. Anal.: C, 8.63; H, 2.99; S, 3.54; Ge, 5.27; Si, 31.27.

General Preparation of Ge Nanocomposites from Molecularly Doped Xerogels. The preparation of each germanium nanocomposite was performed using the same general procedure. A sample of a molecularly doped xerogel (prepared as described above) was ground to a powder and was then placed into an alumina boat. The alumina boat containing the sample was inserted into a quartz tube which was then placed into a tube furnace. The atmosphere within the quartz tube was controlled by passing the desired gas through the tube at a rate of 150 mL/min, and the temperature of the sample was measured via an internal thermocouple placed directly above the sample. When the atmosphere around the sample was changed from air to hydrogen, nitrogen gas was passed through the tube for 5 min before the introduction of hydrogen gas was initiated. Xerogel monolithic pieces appeared clear and colorless following the oxidative thermal treatment. After the reductive thermal treatment, the xerogel slivers were clear and had an auburn color.

Preparation of Germanium Nanocomposite 2b. A 41.8 mg sample of molecularly doped xerogel **2a** was heated from room temperature to 900 °C in air over a period of 2 h. The sample was then heated at 900 °C in hydrogen for 6 h. The xerogel was isolated as a black solid (26.3 mg). Anal.: C, <0.5; H, <0.5; S, <0.3; Ge, 7.39; Si, 40.43.

Preparation of Germanium Nanocomposite 3b. A 40.0 mg sample of doped xerogel **3a** was heated at 600 °C in air for 30 min and then in hydrogen for 1 h. The sample was then heated at 900 °C in hydrogen for 30 min. The xerogel was recovered as dark red xerogel fragments (30.1 mg) which, when viewed under an optical microscope, were transparent. Anal.: Ge, 6.86; Si, 39.17.

Results and Discussion

The preparation of nanocomposites containing nanoclusters of highly crystalline Ge dispersed throughout a bulk silica xerogel matrix is shown in eq 1. Addition

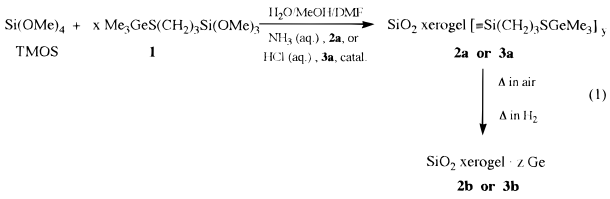

of the organogermanium compound, **1**, to conventional silica xerogel, sol−gel formulations gives silica xerogels **2a** (base catalyst) or **3a** (acid catalyst) doped with the organogermanium fragment. Covalent incorporation of the organogermanium fragment into the silica xerogel matrix is presumed based on the expectation that the Si−OMe groups of both TMOS and the $Si(OMe)_3$ functionality of **1** will undergo catalytic hydrolysis and heterocondensation to form a xerogel matrix. The successful formation of doped xerogels **2a** or **3a** containing controlled relative amounts of organogermanium dopant via systematic variation of the TMOS/**1** reactant stoichiometry is consistent with such covalent incorporation. Furthermore, the thiolate substituent present in **1** has been used by Evans and Gracey as a bifunctional ligand in selected metal carbonyl cluster complexes to achieve covalent attachment of such complexes to the surfaces of metal oxide powders, including silica.[29] This attachment occurs through the heterocondensation of the thiolate $Si(OMe)_3$ group with surface Si−OH groups. Schubert and co-workers have also used $(CH_2)_3Si(OMe)_3$ tethers on amine ligands as a method for obtaining covalent incorporation of amine metal complexes into silica xerogels.[30]

Energy-dispersive analysis (EDS) of the molecularly doped xerogels, **2a** or **3a**, over multiple sites reveals a

(28) Mehrotra, F. C.; Gupta, V. D.; Sukhani, D. *J. Organomet. Chem.* **1967**, *9*, 263.

(29) Evans, J.; Gracey, B. P. *J. Chem. Soc., Dalton Trans.* **1982**, 1123.

(30) Breitscheidel, B.; Zieder, J.; Schubert, U. *Chem. Mater.* **1993**, *3*, 559.

constant Si/Ge atomic ratio that is indicative of homogeneous dispersion of germanium dopant compound throughout the xerogel matrix on the micron scale. Chemical microanalysis of **2a** reveals that while 82% of the thiolate sulfur available in **1** becomes incorporated into the xerogel, only 30% of the available germanium is incorporated into the doped xerogel product when base catalysis is employed. These results indicate a high degree of incorporation of **1** into the xerogel matrix with significant partial leaching of the germanium fragment of **1** from the thiolate tether during gel formation. Similarly, chemical microanalysis of **3a** reveals that under acid catalysis 88% of the available thiolate sulfur and 58% of the available germanium present in **1** become incorporated into the molecularly doped xerogel. Complex **1** is presumably less susceptible to chemical degradation under conditions of acid-catalyzed gel formation.

When a sample of molecularly doped xerogel, **2a**, is heated in air during thermogravimetric analysis (TGA), a single-step weight loss trace is observed centered at 368 °C over the range 230−587 °C. After correction for water loss due to ongoing condensation of the silica xerogel matrix (as determined from TGA analysis of undoped xerogel), a 24.5% weight loss due to decomposition of the molecular dopant is evident. On the basis of chemical microanalytical data, a theoretical weight loss of 24.0% is expected if all carbon, hydrogen, and sulfur is eliminated via air oxidation. The close agreement between predicted and observed weight losses during this thermal treatment is consistent with the degree of dopant incorporation into the xerogel and with essentially complete degradation of the organic portion of the dopant molecule through air oxidation. The characteristic odor of SO_2 is also detected during TGA analysis.

Conversion of the molecularly doped xerogels, **2a** and **3a**, to the respective nanocomposites, **2b** and **3b**, is achieved by heating samples of the xerogel in air to remove the organosulfur component by oxidation followed by heating under a hydrogen atmosphere at conditions sufficient for the reduction of GeO_2 to Ge.[31] Subsequent analysis by transmission electron microscopy (TEM) reveals that Ge nanocluster formation occurs during this thermal treatment (vide infra) and that the average diameter and dispersion of Ge particle sizes is sensitive to dopant concentration, the conditions of the thermal treatment, and the type of catalyst used in preparing the doped xerogel.

For example, nanocomposite **2b** (formed using base catalysis and heating in air at 900 °C for 2 h followed by heating in a hydrogen atmosphere at 900 °C for 6 h) contains highly crystalline spheroidal Ge nanoclusters having diameters in the range 200−3000 Å. Chemical microanalysis indicates a residual carbon and sulfur content below the detection limits of 0.5 and 0.3 wt %, respectively. A more precise determination of residual carbon content was not performed; however, sulfur is not observed in EDS spectra of these Ge nanocomposites. Nanocomposite **3b** (formed using acid catalysis and heating in air at 600 °C for 30 min followed by heating in a hydrogen atmosphere for 1 h at 600 °C and then for 30 min at 900 °C) contains highly crystalline spheroidal Ge nanoclusters having diameters in the range 25−145 Å (average diameter of 67 Å).

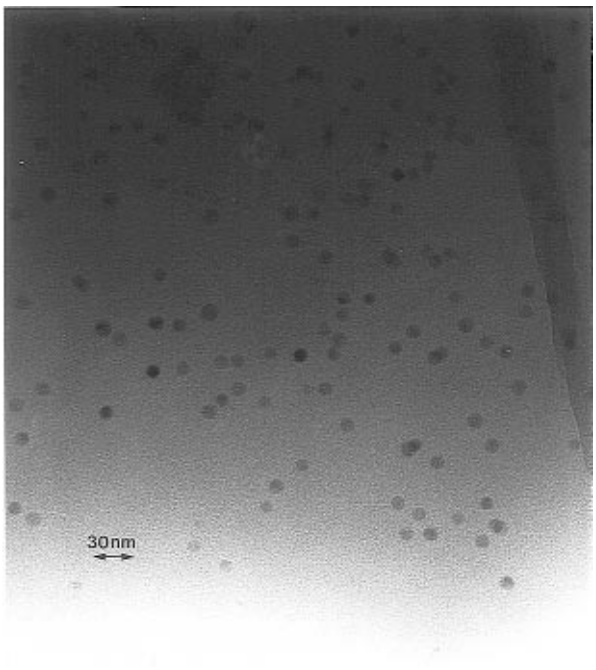

Figure 1. TEM micrograph of silica xerogel nanocomposite, **3b**, containing nanoclusters of Ge.

While the dependence of Ge particle size distribution and average particle size on experimental conditions has not been fully investigated, we observe that smaller and more uniform Ge nanoclusters are obtained from xerogels containing lower doping levels of the molecular precursor **1** that have also been subjected to less rigorous thermal conditions. The nanocomposite sample having the smallest average Ge particle size and the most narrow particle size distribution, **3b**, was therefore chosen for more complete characterization. The preparation of nanocomposite **3b** is found to be very reproducible.

Chemical microanalysis of nanocomposite **3b** indicates a Si/Ge atomic ratio of 15. The observed weight percent of Si (39.17%) is slightly less than that expected for a SiO_2/Ge nanocomposite (43.21% Si) having the same Ge content and is consistent with the presence of residual Si−OH groups and/or absorbed water within the xerogel matrix.

A TEM micrograph of nanocomposite **3b** is shown in Figure 1. Nearly spherical particulate features are dispersed throughout the amorphous silica xerogel matrix. Energy-dispersive spectra (EDS) of selected areas of sample containing either xerogel matrix or a particulate feature indicate that the Ge present in the sample is localized within these particulates. An EDS scan localized on one such particle is shown in Figure 2. X-ray emissions from silicon present in the matrix and from germanium in the particle are clearly evident. X-ray emission from the copper grid of the sample holder is also evident. EDS scans confirm the absence of sulfur within the sample within detection limits. This result is consistent with chemical microanalytical and TGA data. A histogram of the Ge particulate sizes as observed by TEM for 255 particles is shown in Figure 3. The Ge particle size distribution is monomodal over the range 25−145 Å giving an average particle diameter

(31) Vasyutinskii, N. A.; Petrov, G. I.; Sidorenko, A. P.; Ryseua, Y. I. *Zh. Prikl. Khim.* **1968**, *41*, 657.

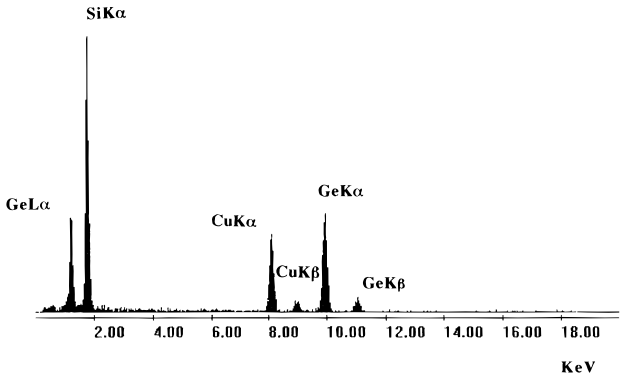

Figure 2. EDS scan (counts vs keV) of a selected area of xerogel containing a particulate feature.

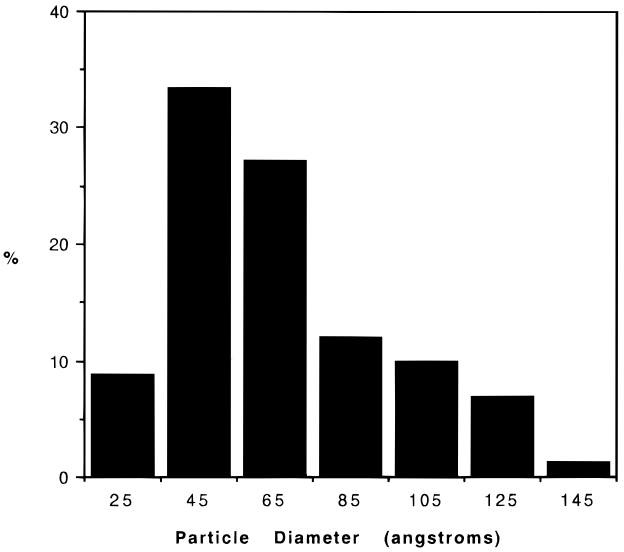

Figure 3. Histogram of the Ge nanocluster particle sizes in nanocomposite **3b** as observed by TEM.

of 67 Å and has a full width at half-maximum (fwhm) value of ca. 40 Å.

Electron diffraction SAD patterns obtained from nanocomposite **3b** reveal three prominent rings each assignable to crystalline germanium [(*hkl* index, actual *d* spacing, Å, observed *d* spacing, Å); (*111*, 3.2667, 3.256); (*220*, 2.0007, 1.983); (*311*, 1.7058, 1.695)]. SAD patterns obtained from nanocomposites prepared from more heavily doped xerogels reveal up to six rings, consistent with crystalline Ge.

A X-ray diffraction (XRD) scan of nanocomposite **3b** is shown in Figure 4 for a rapid scan over 20−60° in 2θ. The broad peak centered near 22° in 2θ is assigned to amorphous scattering from the silica xerogel matrix (as determined from an XRD scan of undoped xerogel). Three peaks matching those expected for crystalline Ge are the only other peaks observed. The *hkl* index, 2θ value (deg), *d* spacing (Å), and angular range (deg) observed for each peak are the following: *111*, 27.49, 3.242, 24.5−30.5; *220*, 45.69, 1.984, 41.8−49.9; *311*, 54.00, 1.700, 50.1−57.6. These three diffraction peaks are also observed by electron diffraction (vide supra). Relative intensities of the *111*, *220*, and *311* diffraction peaks for crystalline Ge are 100, 57, and 39, respectively. A systematic peak shift in the XRD scan is attributed to sample displacement of slightly more than 100 μm from the diffractometer θ axis. A XRD scan of the *311* diffraction peak recorded with a step size of 0.15° in 2θ and a sampling time of 80 s is shown in Figure 4 as an insert. This scan is typical of that recorded for the other two peaks using these better counting statistics. Crystallite sizes calculated from Scherrer's equation using the measured fwhm values of each peak (fwhm in rad, 2θ) [*111* (0.0216), *220* (0.01984), *311* (0.0276)] are 75, 65, and 65 Å, respectively. Contributions to the fwhm from instrumental broadening are negligible compared to the magnitude of the observed fwhm values. The average Ge nanocrystallite size is, therefore, ca. 68 Å. This size is essentially independent of Bragg angle, so within the precision of these measurements, strain broadening

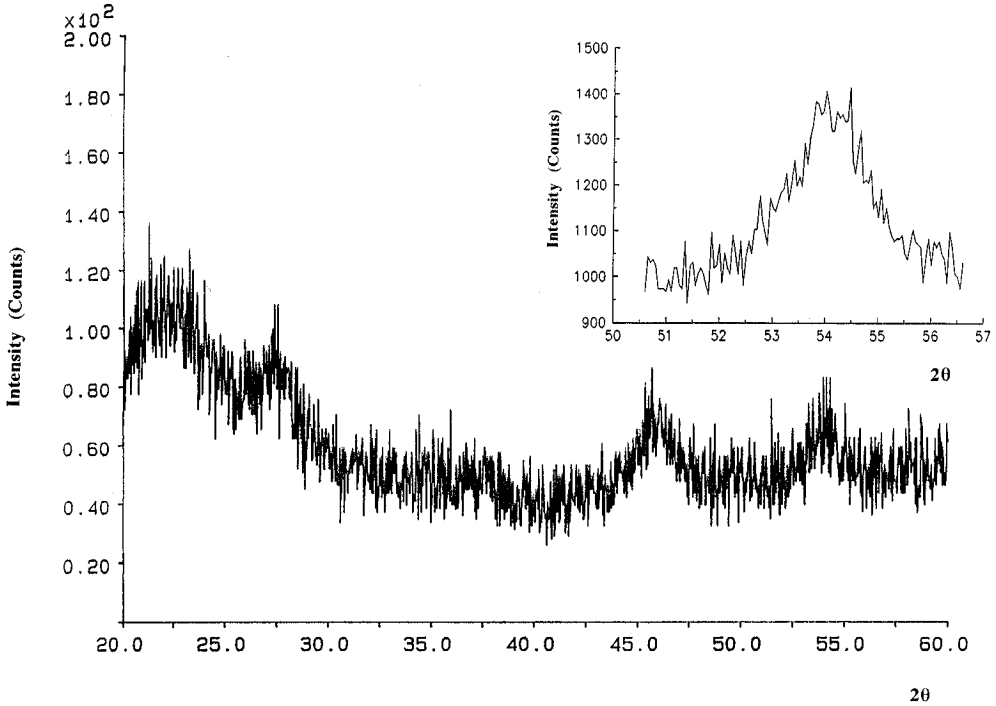

Figure 4. XRD scan of nanocomposite **3b** recorded with Cu Kα radiation (insert shows the XRD scan of the *311* diffraction peak using better counting statistics).

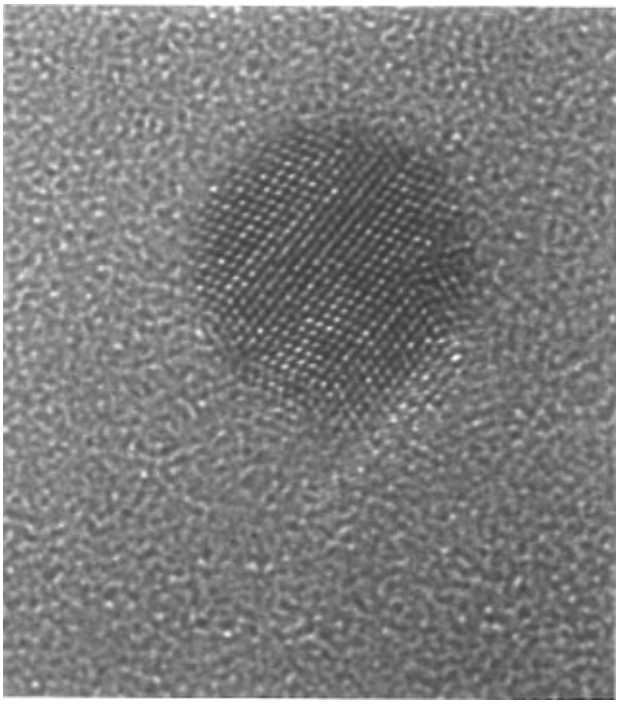

Figure 5. HRTEM micrograph of a typical Ge nanocluster in the nanocomposite **3b**.

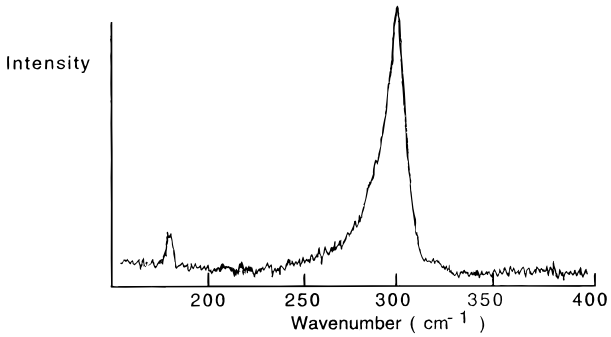

Figure 6. Micro-Raman spectrum of nanocomposite **3b** showing the phonon band of Ge.

effects are not significant. In comparison to the average particle size of 67 Å estimated from TEM micrographs, this value is consistent with high crystallinity of the Ge particles and with the presence of very few crystalline Ge nanoclusters having diameters significantly larger than 145 Å.

The high crystallinity of the Ge particulates is evident in the HRTEM image shown in Figure 5. Two sets of *111* lattice fringes are observed extending across the entire diameter of the nanocluster. The background of the micrograph depicts the amorphous silica xerogel matrix.

A micro-Raman spectrum of nanocomposite **3b** is shown in Figure 6. A sharp signal is observed at 301 cm^{-1} corresponding to the phonon frequency of microcrystalline Ge. The fwhm of this peak of 13 ± 0.5 cm^{-1} is consistent with Ge microcrystals having diameters of ca. 60 Å.[17] Similar Raman signals have been reported and analyzed extensively by Fujii and co-workers for Ge nanoclusters formed in thin films by rf cosputtering methods.[17−19] The presence of a small amount of noncrystalline Ge is evidenced by the trailing of the Ge phonon band to lower frequency. Although neither the Raman signal position nor band width was studied as a function of excitation power, these spectral parameters did not change outside of experimental error during data collection over several hours. This observation suggests that prolonged sample heating effects are not perturbing the observed signal.

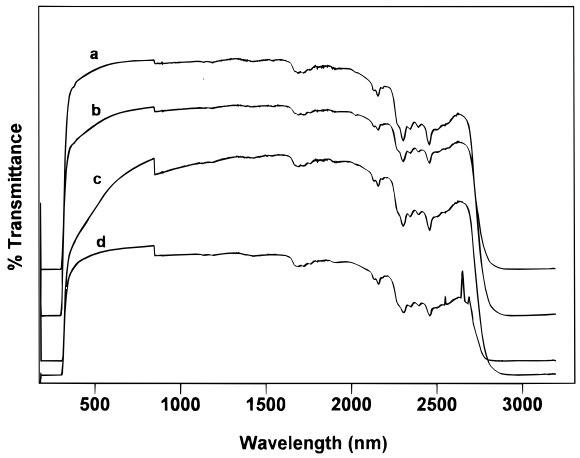

Figure 7. Optical transmission spectra for Ge nanocomposites doped with (a) 1.89×10^{-6} M, (b) 4.73×10^{-6} M, (c) 9.45×10^{-6} M of germanium, and (d) virgin xerogel in an epoxy matrix.

Figure 7 shows transmission optical spectra for the virgin xerogel and for xerogel doped with increasing molar concentrations of germanium. Prominent features are observed in the spectra in the regions 3200−2200 nm for both the doped and undoped xerogel. However, changes in the spectra for the germanium-doped xerogel are most evident in the 1300−350 nm region. At wavelengths shorter than 350 nm, all spectra become saturated.

Within the 1350−350 nm spectral region, the xerogel doped with 9.45×10^{-6} mol of germanium exhibits a gradual decrease in transmittance starting at 1350 nm and ending at 550 nm. The gradual decrease in the transmittance is then followed by a rapidly decreasing transmittance between 550 and 360 nm, which is then followed by a transmittance decrease which has a nearly vertical slope. The spectrum of the xerogel containing 4.73×10^{-6} mol of germanium shows an absorption onset at 550 nm which extends to 360 nm; a much shorter wavelength than the highest dose sample that exhibits an absorption onset at 1350 nm. The slope of the absorption between 550 and 360 nm for the 4.73×10^{-6} mol of germanium sample is considerably less than that of the sample dosed with 9.45×10^{-6} mol of germanium. The lowest dosed xerogel containing 1.89×10^{-6} mol of germanium differs very little from the virgin xerogel and does not seem to have an absorption onset at wavelength longer than 360 nm.

Figure 8 shows derivative optical spectra for the virgin and germanium doped xerogels. As in the case of the transmission spectra, the most conspicuous changes in the derivative spectra are observed in the 550−360 nm region. The samples with 9.45×10^{-6} and 4.73×10^{-6} mol of germanium display a strong peak near 532 nm. This peak is also observed in the 1.89×10^{-6} M sample, but it is much weaker and is not as well defined as it is for the other samples. The remaining portions of the spectra show no significant differences from one another.

The absorptions between 2200 and 3200 and at 1700 nm that are observed in all samples must be due to the

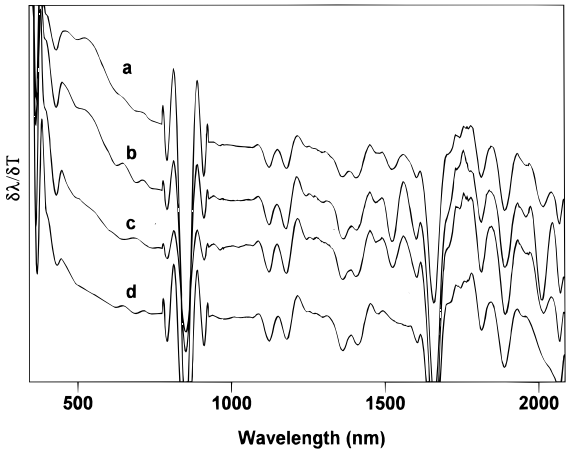

Figure 8. Derivative spectra for Ge nanocomposites doped with (a) 9.45×10^{-6} M, (b) 4.73×10^{-6} M, (c) 1.89×10^{-6} M of germanium, and (d) virgin xerogel in an epoxy matrix.

xerogel and the epoxy used to support the powdered xerogel. The saturation at wavelengths shorter than 350 nm are also expected to be due to absorption by the xerogel and the epoxy matrix. The spectral changes in the 1350−360 nm region are expected to arise from absorptions by germanium nanocrystals. It is noteworthy that for the highest dose sample, a peak is observed in the derivative spectra at 532 nm. This corresponds fairly well with the imaginary part of the dielectric constant for bulk germanium determined from a Kramers−Kronig analysis of the reflectivity of the crystal.[32] The fact that this peak is observed in the spectra of the composite material suggests that band structure is preserved to some extent for the highest dose sample.[19] The highest dose sample also indicates a gradual absorption onset starting at 1350 nm which is well below the bandgap of 1850 nm for the bulk material.[33] For the medium dosing level of 4.73×10^{-6} mol, absorption begins near 550 nm, and for the lowest dose sample no absorption onset could be observed at wavelengths longer than 360 nm. Presumably, the absorption onset for the lowest dose sample must be at a wavelength shorter than 360 nm but could not be observed due the strong overlapping absorption of the xerogel/epoxy matrix.

It is emphasized that no significant absorption is observed at wavelengths between 1850 and 600 nm where bulk germanium is strongly absorbing.[34] The fact that the germanium doped xerogel is transparent in this region suggests that the bandgap is shifted to shorter wavelengths. Also, the general trend observed for the spectra is that the absorption onset is shifted to shorter wavelengths as the dosing level of germanium decreases. Both of these observations are consistent with three-dimensional quantum confinement of the electron−hole system, and therefore we suggest that the changes observed in the optical spectra of these germanium-doped xerogels are in part due to quantum size effects.[35] Experimental and theoretical studies indicate that quantum confinement effects should be evident in germanium nanoclusters within the size domain extending from beyond the molecular scale to particles having diameters not greater than ca. 49 nm.[14,35] The germanium nanoparticles discussed above fall into this size domain.

Conclusions

The organogermanium compound **1** can be incorporated into a silica xerogel matrix using conventional sol−gel formulations. Upon thermal treatment, this molecular dopant acts as a single-source precursor to elemental germanium nanoclusters that are formed highly dispersed throughout the bulk of the xerogel matrix. Independent measurement of the average particle size of these Ge nanoclusters by TEM, XRD, and micro-Raman spectroscopy reveals an average diameter of ca. 68 Å. Features observed in the linear optical absorption spectra of these nanocomposites are consistent with a shift in the bulk Ge bandgap to higher frequencies as expected for Ge quantum dots.

Acknowledgment. C.M.L. thanks Mr. Lloyd Stauffer of Seiko Instruments USA, Inc., for recording TGA measurements. We are grateful to W. J. Reddy, Undergraduate Research Assistant in the School of Materials Science and Engineering, Georgia Institute of Technology, for assistance with XRD measurements. Acknowledgment is made by C.M.L. to the donors of The Petroleum Research Fund, administered by the American Chemical Society, for partial support of this research and to support by, or in part by, the U.S. Army Research Office under Grant DAAH04-95-1-0146. Work performed at Fisk University was supported by NASA under Grant NAG8-1066 (D.O.H.), and work performed at ORNL (J.G.Z.) was supported by DOE under Contract DE-AC05-840R21400 with Lockheed Martin Energy Systems, Inc.

CM950548I

(32) Burst, D.; Phillips, J. C.; Bassani, G. F. *Phys. Rev. Lett.* **1962**, *9*, 94.
(33) Cohen, M. L.; Chelikowsky, J. R. *Electronic Structure and Optical Properties of Semiconductors*; Springer-Verlag: Berlin, 1988; p 45.
(34) Marton, L.; Toots, J. *Phys. Rev.* **1967**, *160*, 602.
(35) Hayashi, R.; Yakamoto, M.; Tsunetomo, K.; Kohno, K.; Osaka, Y.; Nasu, H. *Jpn. J. Appl. Phys.* **1990**, *29*, 756.